Journal of Fluorine Chemistry 213 (2018) 42–50

Contents lists available at ScienceDirect

Journal of Fluorine Chemistry

journal homepage: www.elsevier.com/locate/fluor

The influence of chemical and thermal treatments on the fluoride removal from water by three mineral structures and their characterization

N.G. Corral-Capulin[a,b,c], A.R. Vilchis-Nestor[b], E. Gutiérrez-Segura[c], M. Solache-Ríos[a,*]

[a] Instituto Nacional de Investigaciones Nucleares, Departamento de Química, Carretera México-Toluca S/N La Marquesa, Ocoyoacac, C.P. 52750, Mexico
[b] Centro Conjunto de Investigación en Química Sustentable UAEM-UNAM, Carretera Toluca-Atlacomulco Km. 14.5, San Cayetano, Toluca, Estado de México, Mexico
[c] Facultad de Química, Universidad Autónoma del Estado de México, Paseo Colón esq. Paseo Tollocan, S/N., C.P. 50180, Toluca, Mexico

ARTICLE INFO

Keywords:
Adsorption
Fluoride
Modification
Geomaterials

ABSTRACT

In the present work three different natural materials and their modifications were studied for fluoride removal from aqueous solutions. The materials employed were: clinoptilolite (C), montmorillonite (M) and pumice (P), the minerals were modified with Fe^{3+} and Al^{3+} and heated at temperatures of 200, 500 and 800 °C. They were characterized by thermogravimetric analysis (TGA), differential scanning calorimetry (DSC), X-ray powder diffraction (XRD), scanning electron microscopy (SEM), energy dispersive X-ray spectroscopy (EDS), specific surface area by Branauer Emmett and Teller method (BET) and points of zero charge (pzc). Adsorption experiments were carried out in batch system to obtain the adsorption capacity of each material and evaluate the leaching of iron and aluminum after adsorption processes, throughout the quantification of Fe^{3+} and Al^{3+} in the supernatants. The results obtained indicated the following adsorption capacity order: M (1.008 mg/g) > aluminum-modified materials > iron-modified materials > C > P.

1. Introduction

Nowadays the main sources of drinking water are aquifers as a result of the high levels of pollutants in surface waters like rivers and lakes, mainly in developing countries, the use of groundwater for human consumption has generated several health problems, due to the presence of a significant number of inorganic chemical species, which are transported from soil to aquifers by rainwater, filtration and geochemical processes [1,2]. One of the most abundant constituents of groundwater is fluoride; this element is present in minerals such as: fluorite, apatite and cryolite [3], also in some beverages [4].

The public health problems associated with the presence of fluoride in drinking water occur in many regions of the world and the most affected countries are: India, Sri Lanka, Ethiopia, USA, Mexico, Kenya, Poland and Pakistan [5,6]. Fluoride is considered an essential micronutrient for the maintenance of bones and teeth, especially for children bellow 8 years old, concentrations that exceeds acceptable level of 1.5 mg/L [7], can lead to several diseases and disorders including: dental and skeletal fluorosis, lesions of endocrine glands, thyroid, liver and some other organs, osteoporosis, arthritis and infertility [5,8]. In order to obtain water with the quality and quantity necessary to supply the population demands, several methods have been developed to remove this kind of constituents from water, such as: reverse osmosis, ion exchange, adsorption, coagulation, precipitation and membrane processes [1,9], among them, adsorption is the most extensively used due to its efficiency and economic feasibility [1]. In the last decades a great variety of materials that allow fluoride removal from water have been tested like activated carbon [10], activated alumina, bauxite [11,12], chitin, chitosan [13], metal oxides [14], pumice [2,15], zeolites [16] and modified clays, however, the use of these adsorbents may be limited by sociocultural factors, complex synthetic methods and physicochemical properties [9]. Special attention has been focused on geomaterials due to their low cost, abundance in nature, potential ion exchangers, high surface area, molecular sieve structure, chemical and mechanical stability, surface and structural properties that allow them to be considered as effective adsorbents [17], especially when they are used in their modified form.

In this work, a zeolite of the type clinoptilolite, a clay of the type montmorillonite and pumice were used as adsorbents. These materials have a similar chemical composition but differ in their structure. Clinoptilolite is a hydrated aluminosilicate widely distributed in nature; its structure consists of tetrahedra of Si^{4+} surrounded by oxygen atoms that share their vertices to form three-dimensional networks with channels and well-defined cavities. This material is characterized by a partially negative charge due to the isomorphic substitution of Si^{4+} by Al^{3+}, which is compensated by the presence of exchange cations such

* Corresponding author.
E-mail address: marcos.solache@inin.gob.mx (M. Solache-Ríos).

https://doi.org/10.1016/j.jfluchem.2018.07.002
Received 10 April 2018; Received in revised form 6 July 2018; Accepted 6 July 2018
Available online 07 July 2018

as Na^+, K^+ and Ca^{2+} [18], this property makes it highly functional in processes of ion exchange, catalysis and adsorption [19,20]. Montmorillonite is naturally abundant clay used in the environmental field due to its cation exchange properties [21], it belongs to the smectite family. The members of the smectite family consist of a layered structure composed of a layer of octahedrons attached at the ends of the layer of tetrahedrons that share the oxygen atoms located at the vertices. The octahedral sites are mainly occupied with Al^{3+} and are partially replaced by atoms with lower valence like Mg^{2+} or Fe^{2+}, whereas the tetrahedra are occupied by Si^{4+} and Al^{3+}, causing a deficiency of charge in the structure, which is compensated by the presence of ions such as Na^+ and Ca^{2+} located in the interlaminar space [22]. Pumice is an igneous volcanic rock with low density, considered as an accessible material, due to its availability in nature; it has a pale color in shades ranging from white, cream, gray, blue, green-brown to black, it is mainly formed by silicon oxides, which makes it an abrasive material [5,23]. This rock is formed by the decompression and release of gases from the magma prior to the formation of the glass, which generates a high porosity that can represent up to 90% of its volume [5]. It is widely used in the environmental field as a support material, filter media and adsorbent, due to the silanol groups present on the surface that act as active sites [24]. The properties of these materials make them ideal for the incorporation of new species into their structure, in such a way that they can increase their removal capacities and in turn their affinities for anionic species.

Many methods and chemicals have been applied in the modification of geomaterials. Sun et al., [25] modified a zeolite of the stilbite type with Fe^{3+} using 0.1 M $FeCl_3$ solution in order to improve its surface properties obtaining a maximum fluoride adsorption capacity of 2.31 mg/g. Bia et al., [3] modified a montmorillonite with Fe^{3+} by a precipitation method using a 0.01 M $Fe(NO_3)_3$ solution to obtain a solid with a specific surface area of 567 m^2/g. Asgari et al., [5] used a cationic surfactant to modify pumice; the surfactant used was hexadecyltrimethyl ammonium (HDTMA) and a removal capacity of 41 mg/g was determined. Noori Sepehr et al., [2] compared the defluoridation capacities of a natural pumice (NP), modified with Mg^{2+} (MGMP) and H_2O_2 (HMP), obtaining the following efficiencies order: HMP(11.77 mg/g) > MGMP(5.56 mg/g) > NP(4.53 mg/g) attributed to specific surface areas of 53.11, 41.63 and 2.34 m^2/g, respectively. Malakootian et al., [26] studied the chemical activation of pumice using three different reactants: $FeCl_3$, $Al_2(SO_4)_3$ and hexadecyl trimethyl ammonium bromide (HDTMA-Br) to compare their adsorption efficiencies and the maximum adsorption capacity was 0.29 mg/g with the material modify with HDTMA-Br. Salifu et al. [9] modified a pumice with aluminum oxides by chemical precipitation and the adsorption capacity found was 7.87 mg/g. The development of modified geomaterials offers a viable alternative for the treatment of water containing fluoride. In this way, many works have reported that geomaterials impregnated with divalent and trivalent metal ions helps to increase their defluoridation capacities according with the concept of hard and soft acids and bases [9,27]. The defluoridation efficiencies of metal-modified materials are shown in the following order: $La^{3+} \geq Ce^{3+} > Y^{3+} > Fe^{3+} \sim Al^{3+} > Ca^{2+} > Mg^{2+} > Zn^{2+}$ [28] also the works by Salifu et al., [9] and Gomoro et al., [29] suggested that thermal treatments offer stability to the geomaterial structure through the metal oxidation process. In the present work Fe^{3+} and Al^{3+} were used as hard acids for the chemical treatment of clinoptilolite, montmorillonite and pumice, furthermore, the natural and metal modified-materials were heated at three different temperatures to evaluate their ability to remove fluoride from water solutions, also iron and aluminum leaching were study to determine their stability in the materials and avoid their release into the remaining solutions after the adsorption processes.

2. Experimental

2.1. Materials

Clinoptilolite (C) was obtained from Etla, Oaxaca, Mexico, pumice stone (P) was supplied from a mine located in Hidalgo, México and montmorillonite (powder) (M) was obtained from Fluka (Sigma-Aldrich). The chemicals NaCl, $FeCl_3{\cdot}6H_2O$, $AlCl_3{\cdot}6H_2O$, NaOH, HCl and NaF were from J.T. Baker.

2.2. Chemical treatment

Clinoptilolite and pumice rocks were crushed and sieved between 20 and 40 mesh to obtain homogeneous particle sizes between 0.84 and 0.42 mm, the solids were washed with distilled water and dried at room temperature. Subsequently, the three materials were conditioned with 1 M NaCl solution under reflux for 6 h in order to guarantee the exchange of the natural cations by Na^+. The phases were separated by decantation; the solids were washed with distilled water until the materials were free of chloride ions (Cl^-) that was observed by AgCl test. Finally, they (C-Na, M-Na and P-Na) were dried at 50 °C for 24 h.

The chemical treatments with Fe^{3+} were performed based on the work reported by Guaya et al. [30] using a 0.2 M $FeCl_3$ solution, which was contacted with C-Na, M-Na and P-Na under the same conditions as the NaCl solution treatment. The materials were identified as C-Fe, M-Fe and P-Fe.

The Al^{3+} modifications were carried out by chemical precipitation, using the method reported by Vázquez Mejía et al. [31] putting in contact sodium-modified materials (C-Na, M-Na and P-Na) with a 0.2 M $AlCl_3{\cdot}6H_2O$ solution. The suspensions obtained were stirred at 100 rpm and a 5 M NaOH solution was added until a pH of 8 was reached. The suspension was kept under stirring for 5 h, then the phases were separated by decantation and the solids were washed with distilled water and dried at 50 °C for 24 h. The materials obtained were labeled as C-Al, M-Al and P-Al.

2.3. Thermal treatment

Natural and modified materials with Fe^{3+} and Al^{3+} were heated at 200, 500 and 800 °C in a Lindberg muffle for 1 h. The materials obtained were identified as: C-200, C-500, C-800, M-200, M-500, M-800, P-200, P-500, P-800, C-Fe 200, C-Fe 500, C-Fe 800, M-Fe 200, M-Fe 200, M-Fe 500, M-Fe 800, P-Fe 200, P-Fe 500, P-Fe 800, C-Al 200, C-Al 500, C-Al 800, M-Al 200, M-Al 500, M-Al 800, P-Al 200, P-Al 500 and P-Al 800. The materials were stored in a moisture-free place.

2.4. Characterization

The analytical techniques used for characterization of the materials are fundamental to determine the types of interactions between adsorbate and adsorbent in adsorption processes.

2.4.1. Thermogravimetric analysis (TGA) and differential scanning calorimetry (DSC)

Thermal analysis of the samples: C-Fe, M-Fe, P-Fe, C-Al, M-Al y P-Al were carried out using a TA-instrument Q600. The samples were heated up to 650 °C in an alumina crucible with the following operating conditions: 10 °C/min in nitrogen atmosphere.

2.4.2. X-ray powder diffracción (XRD)

XRD patterns were obtained through a diffractometer D8 ADVANCE, BRUKER, under the following conditions: range of 5–75 2Θ, step of 0.03, voltage and current of the tube 35 kV and 35 mA, respectively.

2.4.3. Infrared spectroscopy (FTIR)

Analysis by FTIR of the samples: C, C-Na, C-Fe, C-Fe 200, M, M-Na, M-Fe, M-Fe 200, P, P-Na, P-Fe y P-Fe were carried out in the interval of 4000 to 400 cm^{-1} by using a spectrometer Bruker Tensor 27 with attenuated total reflection (ATR) accessory model platinum.

2.4.4. Scanning electron microscopy (SEM) and energy dispersive X-ray spectroscopy (EDS)

The study of the morphology of natural and modified materials was performed using a scanning electron microscope JEOL JSM-6610LV at low vacuum. Elemental semi-quantitative analyzes of the materials were performed by energy dispersive X-ray spectroscopy (EDS).

2.4.5. Specific surface area by branauer emmett and teller method (BET)

Determination of the specific surface area was performed by the Branauer-Emmett-Teller method (BET), through nitrogen adsorption isotherm using a Belsorp-max equipment, BEL JAPAN INSTRUMENTS, prior to the analysis the samples were degassed in a Belprep II equipment at 200 °C for 2 h.

2.4.6. Point of zero charge (pzc)

Determination of the pzc was carried out for the samples C-Fe, C-Fe 200, M-Fe 200, M, C-Al 200 and P-Al 200. Different pH values were tested from 1 to 12, the pH adjustment was performed with 0.1 M NaOH or HCl solutions using a pH meter PHM290, pH-stat controller Copenhagen. The experiments were done in duplicate by contacting 0.1 g of each material with 10 mL of 0.1 M NaCl solution with different pH (from 1 to 12) for 48 h with constant shaking at 120 rpm and temperature of 30 °C. The final pH of the solutions was measured and plotted against the ΔpH (difference of the equilibrium pH and the initial pH ($\Delta pH = pH_e - pH_i$)).

2.5. Adsorption

After chemical and thermal treatments, 39 materials were obtained and their ability to remove fluoride from water was evaluated. The removal processes consisted of contacting 0.1 g of each material with 10 mL of 10 mg/L F^- solution at 30 °C and 120 rpm for 72 h. After the adsorption processes, iron and aluminum concentrations were determined in the remaining solutions by atomic absorption spectroscopy (AA) and inductively coupled plasma mass spectrometry (ICP-MS), respectively.

2.6. Fluoride measurements

The quantification of fluoride in aqueous solution was carried out with a selective ion electrode according to the procedure reported by Velázquez-Peña et al., [32], using a pH meter PHM290, pH-stat controller Copenhagen. Prior to the analysis, a total ionic strength adjusting buffer (TISAB) and 0.1 M KNO_3 solution were added to the samples and standards to control the pH and eliminate the interferences of complexing ions.

3. Results and discussion

3.1. Thermogravimetric analysis (TGA) and differential scanning calorimetry (DSC)

Thermal analyzes indicated that the decomposition of the materials C-Fe, C-Al, M-Fe and M-Al was carried out in three stages. According to the thermograms in Fig. 1, the first stage is associated with a loss of weight due to dehydration processes or by desorption of water molecules located on the surfaces of the materials, which are weakly bound. The second stage is attributed to the loss of water of crystallization; molecules that are coordinated to the exchangeable cations within the structure of the clinoptilolite and in the interlayer spaces of the montmorillonite. Finally, the third stage is associated with the dehydroxylation process, a phenomenon that causes the release of hydroxyl groups from the structures of the minerals [23,33,34].

In the cases of P-Fe and P-Al (Fig. 1c and f), thermal decompositions take place in two stages, the first one is associated with the dehydration process and the second one was attributed to the dehydroxylation phenomenon (Table 1). According to the results obtained by DSC, these processes are chemical and endothermic in nature [35]. According with these results, the temperatures for thermal treatments were established at: 200, 500 and 800 °C, where the main losses of weights take place (Table 1).

3.2. X-ray powder diffracción (XRD)

XRD patterns were used for the structural analysis of the samples C, M y P. Fig. 2a (C) shows that zeolitic rock is mainly composed by the crystalline phases clinoptilolite, mordenite and quartz. Clinoptilolite was identify by the presence of diffraction peaks at 9.87°, 11.17°, 22.35° and 30.8° on the 2-Theta axis (JCPDS 47-1870), while mordenite was characterized by the diffraction peaks at 6.47°, 8.93°, 13.45°, 15.2°, 19.58°, 25.61°, 27.67°, 30.9° and 35.63° (JCPDS 60-0847). Finally, quartz was identified by the peak at 26.6° (JCPDS 01-0649).

Fig. 2b shows the XRD pattern of the clay (M), the sample is mainly composed by the crystalline phases: muscovite, montmorillonite and quartz. Muscovite is characterized by the diffraction peaks at 8.84°, 17.73°, 22.90°, 23.84°, 26.59°, 27.76°, 31.14°, 34.88°, 37.77°, 42.4° and 61.8° on the 2-Theta axis (JCPDS 46-1045), while montmorillonite was identified by peaks at 6.29° and 19.82° (JCPDS 03-0014). The quartz content was identified with the diffraction peaks at 20.86°, 26.64° and 50.13° on 2-Theta (JCPDS 000-0 46-1045). The diffractogram of pumice, Fig. 2c, shows that the material is composed mainly by amorphous phases, this is due to the process of rock formation, where the atoms that constitute this material are distributed randomly as a result of the rapid decrease in temperature and decompression of the magma that emerges from the volcanic crater, however, the diffractogram obtained is characteristic of this type of rock that is mostly constituted of SiO_2 [23]. Nevertheless, it is possible to observe the presence of peaks with high intensity at 27.95, 29.6 and 47.72° that correspond to albite phase.

Fig. 2a and b, shows that the diffractograms of materials conditioned with Na^+ and Fe^{3+} do not suffer significant variations in the positions and intensities of the main peaks compared to the diffraction patterns of natural materials (C and M), therefore, the treatments do not generate structural changes, however, the intensity of the peak associated with quartz in 26.6° on the 2-Theta axis shows a decrease in its intensity for the materials C-Na and C-Fe.

After thermal treatment of the modified clinoptilolite samples a decrease in the intensity of the peaks associated with the mordenite was observed, which may indicate that this crystalline phase is less stable as a function of temperature compared with clinoptilolite, where no significant changes were observed in their diffraction peaks. In the case of the materials M-Fe 200, M-Fe 500 and M-Fe 800 a slight decrease in the intensity of the peak at 6.29° was observed and it was progressively from 200 to 800 °C, as a result of the loss of water molecules, this diffraction peak refers to the interlaminar space of the clay, and the literature suggests that an increase in the temperature causes a widening of the interlaminar space, and therefore, the intensity of the peak decreases.

3.3. Infrared spectroscopy (FTIR)

Fig. 3a shows the infrared spectra for the samples C, C-Na, C-Fe and C-Fe 200, a wide band with a high intensity is observed at 1043 cm^{-1} associated to asymmetric stretching vibrations of Si-O bond of the tetrahedra SiO_4, in addition the bands at 797 and 460 cm^{-1}, were assigned to stretching and bending vibrations of O-Si-O groups [36], and

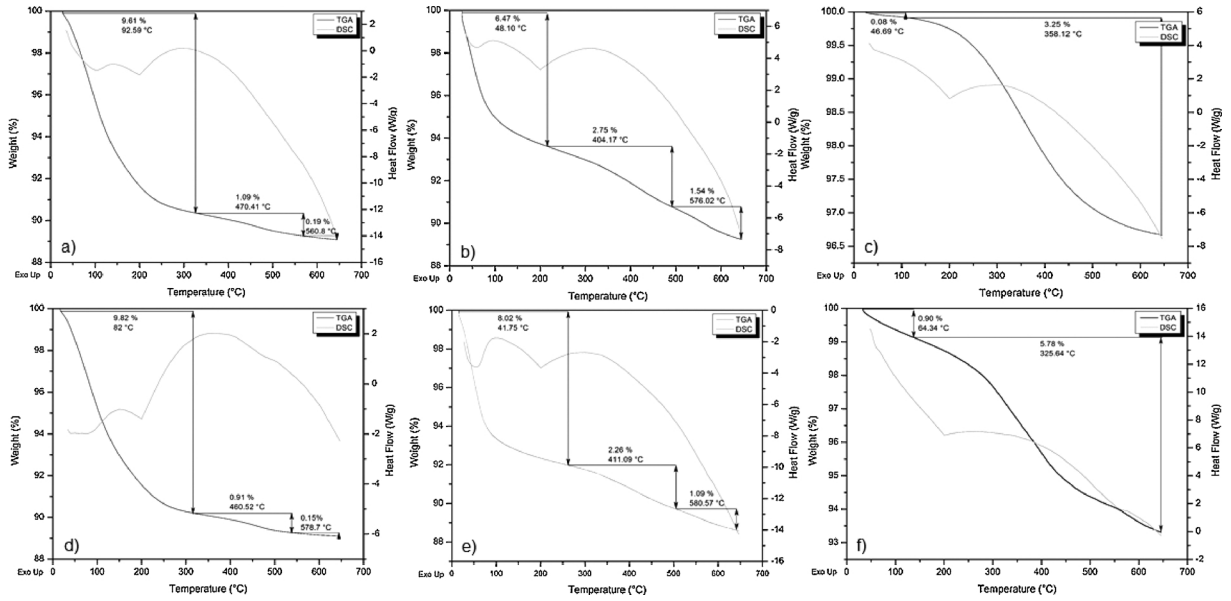

Fig. 1. TGA and DSC curves: a) C-Fe, b) M-Fe, c) P-Fe, d) C-Al, e) M-Al and f) P-Al.

Table 1
Results by TG/DCS analysis.

Material	Stage 1			Stage 2			Stage 3		
	% TG	T (°C)	DSC	%TG	T (°C)	DSC	%TG	T (°C)	DCS
C-Fe	9.61	92.59	Dehydration Endothermic	1.09	470.41	Loss of water of crystallization Endothermic	0.19	560.8	Dehydroxilation Endothermic
C-Al	9.82	82.00	Dehydration Endothermic	0.91	460.52	Loss of water of crystallization Endothermic	0.15	578.7	Dehydroxilation Endothermic
M-Fe	8.02	41.75	Dehydration Endothermic	2.26	411.09	Loss of water of crystallization Endothermic	1.09	580.57	Dehydroxilation Endothermic
M-Al	6.47	48.10	Dehydration Endothermic	2.75	404.17	Loss of water of crystallization Endothermic	1.54	576.02	Dehydroxilation Endothermic
P-Fe	0.08	46.69	Dehydration Endothermic	3.25	358.12	Dehydroxilation Endothermic	–	–	–
P-Al	0.90	64.34	Dehydration Endothermic	5.78	325.64	Dehydroxilation Endothermic	–	–	–

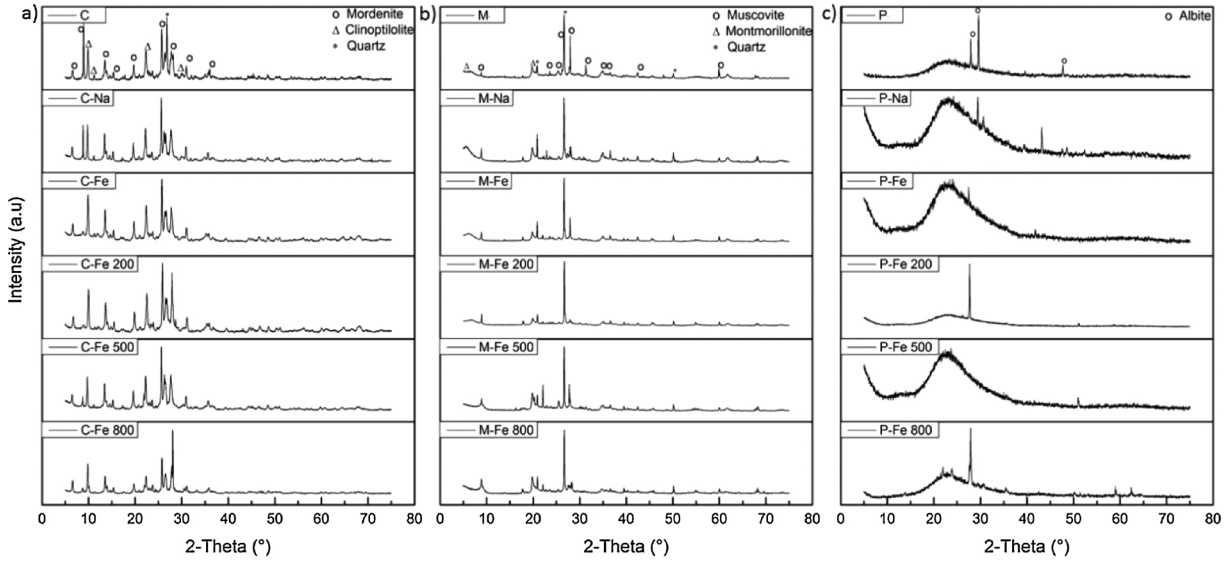

Fig. 2. XRD patterns: a) natural clinoptilolite and modifications, b) natural montmorillonite and modifications and c) natural pumice and modifications.

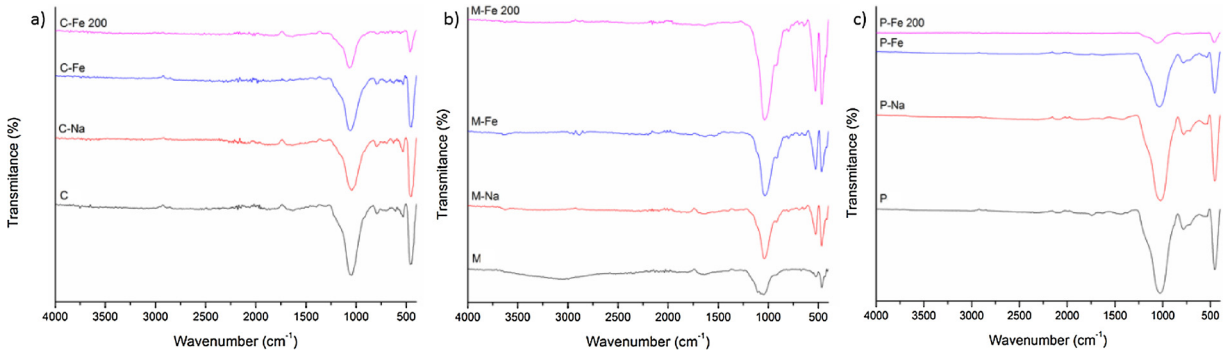

Fig. 3. Infrared Spectra: a) C, C-Na, C-Fe and C-Fe 200, b) M, M-Na, M-Fe and M-Fe200.

the 460 cm^{-1} signal to the vibration of Si-O-Fe bond. The band at 608 cm^{-1} is attributed to the bending vibrations of the Al-O-Si bonds [37]. After chemical treatments, the signal at 460 cm^{-1} shows variations in its intensity, a phenomenon that is attributed to the presence of Fe^{3+} species. In addition, after the heating treatment, this signal presents a remarkable decrease in its intensity associated with the loss of water of hydration linked to Fe^{3+}, causing the formation of oxides and giving greater stability to the sample [36].

Fig. 3b shows the IR spectra of M, M-Na, M-Fe and M-Fe 200 samples. The signals at 1060 cm^{-1} correspond to the asymmetric stretching vibration of the Si-O bond of the SiO_4 tetrahedron layers, the peak at 916 cm^{-1} represents the bending vibration of the Al−OH bond [38], the stretching and bending bands of the O-Si-O bonds are observed at 797 and 460 cm^{-1}, respectively [36] and the absorption band at 520 cm^{-1} is associated to the bending vibration of the Si-O-Mg group [38]. In addition, the absorption bands at 3600 and 1643 cm^{-1} represent the stretching and bending vibrations of the OH group [39]. The absorption bands at 460 and 520 cm^{-1} increase in intensity after each modification, this behavior can be attributed to the presence of new chemical species.

Pumice infrared spectra (Fig. 3c) shows an adsorption band at 1029 cm^{-1} corresponding to the asymmetric stretching vibration of the Si-O bond characteristic of aluminosilicates. At 783 and 457 cm^{-1} stretching and bending bands of the O-Si-O bonds are observed.

3.4. Scanning electron microscopy (SEM) and energy dispersive X-ray spectrometry (EDS)

Fig. 4 shows SEM images of the sample C, that describes the typical morphology of a sedimentary zeolite which occurred as euhedral plates and laths and is characterized by a monoclinic structure, this sample presents a rough surface with cavities and crystals with shape of a cube or coffin [32]. M is composed by agglomerates of particles of variable size lacking a defined morphology. P shows a rough texture due to the presence of a system of pores and cavities of heterogeneous size, it has the characteristics of a highly abrasive material. Moreover, SEM images of the iron and aluminum-modified materials show that they conserve their morphological features after chemical treatments. However, for the case of the aluminum-modified materials the presence of small particles on their surfaces was observed, which are not appreciable in natural materials and iron-modified ones. Therefore, the presence of Al $(OH)_3$ can be attributed to the modification with Al^{3+} by chemical precipitation. Fig. 4 shows that iron and aluminum are distributed homogeneously on the surface of the minerals.

EDS analysis of the natural, sodium, iron and aluminum-modified materials are reported in Tables 2–4. Natural materials are constituted mainly by O, Si and Al, each mineral presents variations in its composition; C shows the presence of Na, K and Ca, while P shows Na and K, these elements are considered as exchangeable ions that naturally occurs in the mineral structures. M shows variable composition containing elements like S and Ti that are considered impurities; Ca and K were also identified as exchangeable cations. After each chemical treatment, the amounts of sodium, iron and aluminum increase which indicates that every treatment allow the incorporation of these species to the mineral structures. Finally, the presence of Cl has been identified in C-Fe and C-Al, which is associated to the chemical nature of the precursors used for the modifications and were not totally removed during the washing stages.

3.5. Specific surface area by Branauer Emmett and Teller method (BET)

The specific surface area, total pore volume and mean pore diameter of the samples are shown in the Table 5. The results indicate that the mean pore diameter of the samples is within the range of 2–50 nm, according to IUPAC classification these values correspond to mesoporous materials. This size range favors the diffusion of fluoride in the internal structure of the materials taking in consideration that its ionic radius is 1.33 Å. Regarding surface areas, clinoptilolite and montmorillonite modified materials increase this parameter after each chemical treatment, as a result of the removal of particles or impurities that are obstructing the pores and cavities of the materials. In addition, iron-modified materials have the largest surface areas (about 300 m^2/g), which can be attributed to the presence of iron hydroxides and oxides like ferrihydrite, these values agree with the results reported by Borgino et al. [40], who explain that the creation of large quantities of new functional groups and adsorption sites could increase the adsorption capacity.

BET analysis were performed on C-Fe 200, C-Fe 500 and C-Fe 800 samples with the purpose of determining the effect of thermal treatment on their textural properties, the results reveal that specific surface areas decrease with increasing the temperature of thermal treatment, this behavior obeys a reduction in the amount of hydroxyl groups as a result of the loss of hydration, crystallization and structural waters, as observed by TG and DSC analysis, this phenomenon can also be associated to the internal changes in the structures and for the samples heated at 800 °C a collapse could occur, as well by agglomeration of oxide particles of Fe^{3+} or Al^{3+} [41]. In addition, the total pore volume is proportional to the specific area, decreasing with the increase of temperature, which can be attributed to a reticular movement of the molecules due to the replacement of the compensation ions with valence of +1 and +2, by Fe^{3+} and Al^{3+}. Finally, it can be highlighted that the sample P-Al 200 showed the lowest surface specific area and pore volume, which could have a negative impact on its removal capacity.

3.6. Point of zero charge (pzc)

Among the main properties of materials is the pzc because it indicates the protonation and deprotonation reactions on the surfaces of the solids in aqueous solution and the interaction between adsorbate

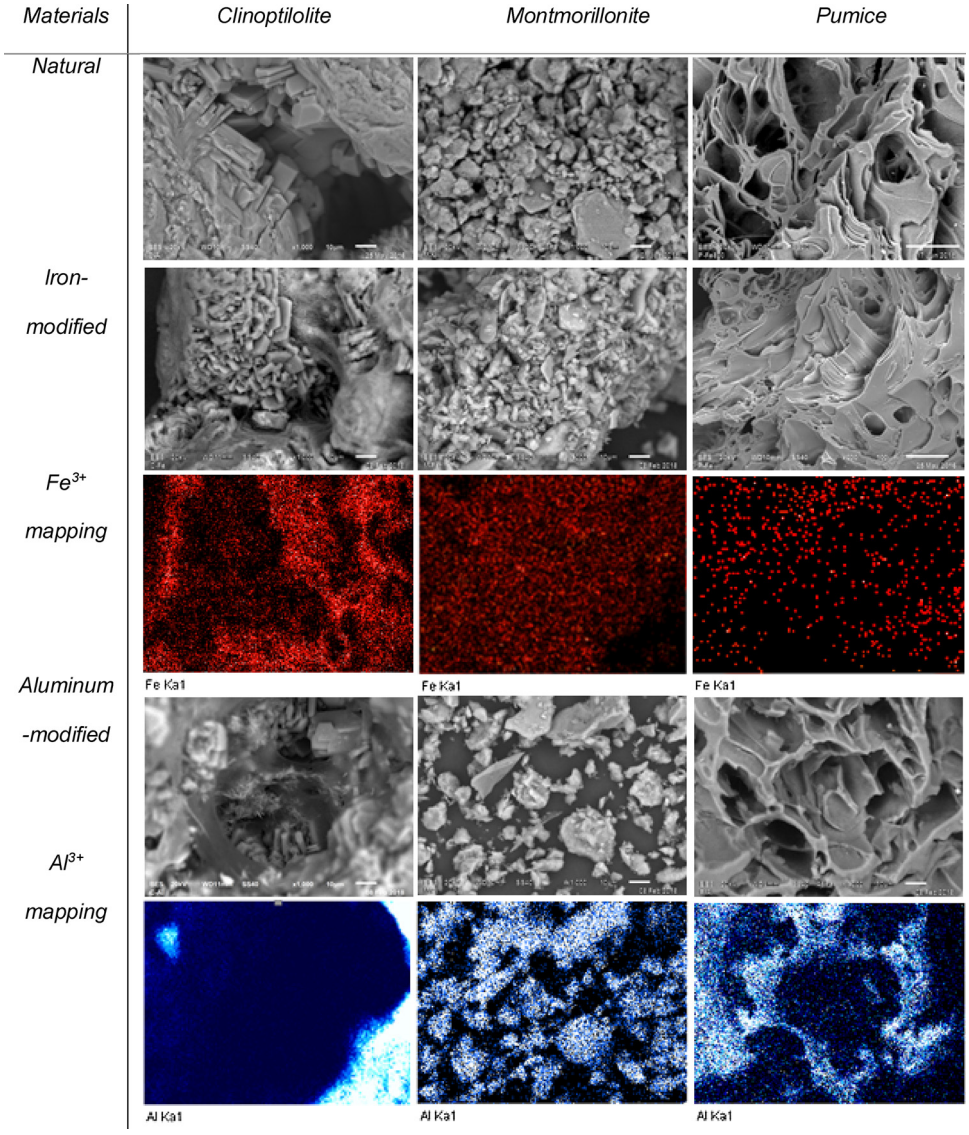

Fig. 4. SEM analysis.

Table 2
Chemical composition (wt %) of the samples: C, C-Na, C-Fe and C-Al.

Element	Material			
	C	C-Na	C-Fe	C-Al
O	49.53 ± 1.41	48.15 ± 1.94	46.18 ± 2.86	50.35 ± 1.45
Na	3.27 ± 0.18	3.80 ± 0.35	1.44 ± 0.36	2.44 ± 0.44
Al	6.67 ± 0.17	7.37 ± 0.44	5.95 ± 1.29	17.96 ± 2.62
Si	37.54 ± 1.34	37.77 ± 1.22	29.92 ± 3.55	25.76 ± 2.72
Cl	–	–	1.12 ± 0.47	2.08 ± 0.61
K	1.61 ± 0.13	1.48 ± 0.25	0.99 ± 0.63	0.72 ± 0.21
Ca	0.57 ± 0.10	0.28 ± 0.08	0.19 ± 0.14	0.17 ± 0.06
Fe	0.81 ± 0.34	1.15 ± 0.71	14.21 ± 4.82	0.52 ± 0.17

Table 3
Chemical composition (wt %) of the samples: M, M-Na, M-Fe and M-Al.

Element	Material			
	M	M-Na	M-Fe	M-Al
O	46.31 ± 3.23	42.41 ± 0.83	39.49 ± 2.95	46.81 ± 2.06
Na	0.14 ± 0.06	0.30 ± 0.05	0.23 ± 0.05	1.01 ± 0.51
Mg	1.46 ± 0.62	1.31 ± 0.24	1.41 ± 0.73	0.77 ± 0.37
Al	9.12 ± 2.13	10.86 ± 0.38	10.03 ± 3.15	13.84 ± 1.47
Si	27.66 ± 6.20	36.56 ± 1.14	37.92 ± 5.61	33.47 ± 5.54
S	4.73 ± 2.49			
K	2.74 ± 1.66	2.09 ± 0.11	1.38 ± 0.64	3.36 ± 2.57
Ca	1.04 ± 0.54			
Ti	0.26 ± 0.10	0.55 ± 0.21	0.34 ± 0.22	
Fe	3.89 ± 2.35	6.04 ± 0.73	7.89 ± 2.39	2.55 ± 1.62

and adsorbent in adsorption processes. The results obtained from the experimental tests are presented in Table 6. pH values equal to the pzc materials indicates neutral surface charge, at lower pH values than pzc, the surface of the material acquires a positive charge as a result of the protonation reactions of the hydroxyl groups present in the structures of the materials [30] and at higher pH values than the pzc, solid surface acquires a negative charge as a result of the deprotonation reactions [8]. The values of pzc of the materials C-Fe, C-Fe 200, M-Fe 200 and M are acidic, the solution of $Fe(Cl)_3$ during the chemical modification had pH values lower than one. In the case of aluminum modified-materials, the values of pzc increase considerably, due to the formation of $Al(OH)_3$ during the chemical treatments. Therefore, adsorption processes onto materials like C-Al 200 and P-Al 200, might be attributed to electrostatic interactions, and the removal of fluoride ions could be favored.

Table 4
Chemical composition (wt %) of the samples: P, P-Na, P-Fe and P-Al.

Element	Material			
	P	P-Na	P-Fe	P-Al
O	54.34 ± 5.85	45.27 ± 3.26	39.51 ± 3.37	43.66 ± 1.13
Na	1.29 ± 0.05	1.68 ± 0.28	1.13 ± 0.36	1.09 ± 0.11
Al	5.74 ± 0.29	7.18 ± 0.27	10.56 ± 5.36	13.47 ± 1.85
Si	32.05 ± 4.20	37.08 ± 2.57	37.84 ± 2.06	32.88 ± 2.99
K	6.35 ± 2.11	6.60 ± 1.32	6.67 ± 1.72	1.18 ± 0.58
Fe	1.07 ± 0.58	0.76 ± 0.44	3.20 ± 3.50	6.56 ± 0.58

Table 5
Surface area, total pore volume and mean pore diameter.

Materials	Sample	$a_{S,BET}$ (m^2/g)	V_{poro} (cm^3/g)	Mean pore diameter (nm)
Clinoptilolite	C	20.09	6.58×10^{-2}	13.11
	C-Na	37.45	0.0079	8.47
	C-Fe	224.14	0.1531	2.73
	C-Fe 200	221.33	0.1561	2.82
	C-Fe 500	181.76	0.1426	3.14
	C-Fe 800	89.41	0.1009	4.52
	C-Al 200	20.75	0.0065	12.53
Montmorillonite	M	117	0.0023	11.05
	M-Na	121.28	0.1399	4.27
	M-Fe	130.98	0.1322	4.14
Pumice	P-Al 200	3.99	0.0004	3.52

Table 6
Point of zero charge.

Materials	C-Fe	C-Fe 200	M-Fe 200	M	C-Al 200	P-Al 200
Pcc	2.08	1.96	2.39	2.18	5.12	6.57

3.7. Adsorption

The 39 samples modified with Na^+, Fe^{3+} and Al^{3+} and thermally treated were used to remove fluoride from aqueous solution and to evaluate their efficiencies. The results obtained are shown in Table 7, for the clinoptilolite-based materials, adsorption capacities increase with chemical modifications, iron and aluminum modified materials showed the highest efficiencies, this fact can be attributed to the high affinity of the metals (hard acids) with fluoride (hard base) for the formation of complexes [27], the amount of fluoride ions removed tends to decrease with increasing the heating temperature of samples due to the decrease of surface areas (Table 5), this phenomenon has been described by Biswas et al., [42] who associated it to the compaction or elimination of pores during heating and Gomoro et al., [29] explain that loss of OH groups favors the formation of metal oxides. When the surface is hydrated, surface hydroxyl groups are present. The hydroxyl ions may coordinate with Fe^{3+} and Al^{3+} ions and constitute the functional groups that participate in fluoride removal; C-Fe and C-Al have a higher adsorption capacity in comparison with the samples heated. Also, Salifu et al. [9] reported that interactions between adsorbate and adsorbent highly depends on the point of zero charge, they proposed the following possible interactions:

Protonation and deprotonation reactions as a function of the point of zero charge:

$$MOH + H^+ \leftrightarrow MOH_2^+ \text{ protonated species pH<pzc}$$

$$MOH \leftrightarrow MO^- + H^+ \text{ deprotonated species pH > pzc}$$

Possible interactions between functional groups of iron or aluminum-modified materials with fluoride ions.

$$MOH_2^+ + F^- \leftrightarrow MOH_2^+\text{-}F \text{ electrostatic interaction}$$

$$MOH_2^+ + F^- \leftrightarrow MF + H_2O \text{ exchange reaction}$$

The above reactions describe the possible interactions between metal ions with fluoride. The first one suggests the electrostatic attraction of the anion to the protonated species and is called specific adsorption, while the second describes the ion exchange between the hydroxyl group and fluoride, so-called non-specific adsorption [9].

The materials that showed the highest efficiencies were C-Fe, C-Fe 200, C-Al 200, M, M-Fe 200 and P-Al 200 from the 39 prepared adsorbents. According with the results shown in Table 6, pzc values of the iron modified materials and M are acid, this feature indicates that the removal of fluoride occurs by electrostatic attraction, while adsorption onto C-Al 200 and P-Al 200 can take place by exchange reactions or by a synergistic contribution of both electrostatic attraction and ion exchange processes, this behavior can be responsible for the higher adsorption capacity of aluminum-modified materials than iron-modified ones. Aluminum-modified materials showed a lixiviation of Al^{3+}, after adsorption processes, the quantity of aluminum measurement in the remaining solutions was higher than 0.2 mg/L in all cases; this value is similar to the maximum level of aluminum in drinking water recommended by World Health Organization (WHO) [7]. The high aluminum content in the remaining solutions could be due to the formation of $Al(OH)_3$ which do not have chemical interactions with the matrices, contrary to the iron-modifies materials, where Fe^{3+} is incorporated in the structure of the minerals and the concentration of Fe^{3+} in the remaining solutions was lower than the maximum level of 0.3 mg/L in drinking water established by WHO.

The behavior of the montmorillonite-base materials was different from that observed with the clinoptilolite, in this case the natural

Table 7
Adsorption capacities of fluoride ions by natural and modified materials. Concentration of iron and aluminum in the remaining solutions after adsorption processes.

Clinoptilolite				Montmorillonite				Pumice			
Material	q (mg/g)	Fe^{3+} (mg/L)	Al^{3+} (mg/L)	Material	q (mg/g)	Fe^{3+} (mg/L)	Al^{3+} (mg/L)	Material	q (mg/g)	Fe^{3+} (mg/L)	Al^{3+} (mg/L)
C	0.050	–	–	M	1.008	–	–	P	0.012	–	–
C-200	0.032	–	–	M-200	1.010	–	–	P-200	0.000	–	–
C-500	0.000	–	–	M-500	1.007	–	–	P-500	0.000	–	–
C-800	0.000	–	–	M-800	0.177	–	–	P-800	0.259	–	–
C-Na	0.183	–	–	M-Na	0.556	–	–	P-Na	0.018	–	–
C-Fe	0.773	0	–	M-Fe	0.599	0	–	P-Fe	0.034	0.03	–
C-Fe 200	0.733	0	–	M-Fe 200	0.685	0	–	P-Fe 200	0.000	0	–
C-Fe 500	0.542	0	–	M-Fe 500	0.508	0	–	P-Fe 500	0.000	0	–
C-Fe 800	0.003	0	–	M-Fe 800	0.187	0	–	P-Fe 800	0.000	0	–
C-Al	0.959	–	0.81	M-Al	0.312	–	2.41	P-Al	0.848	–	0.87
C-Al 200	0.888	–	0.51	M-Al 200	0.325	–	3.71	P-Al 200	0.802	–	0.47
C-Al 500	0.574	–	0.62	M-Al 500	0.192	–	3.30	P-Al 500	0.445	–	1.03
C-Al 800	0.019	–	0.56	M-Al 800	0.112	–	2.96	P-Al 800	0.392	–	5.67

material (M) presents a higher efficiency compared to the modified ones, a phenomenon that can be associated with the loss of crystalline phases of the original material during the treatments, the presence of calcium oxides was reduced (Table 4), Ca could participate forming complexes with the fluoride ion, because within the Pearson classification it is also considered a hard acid. In general, the modified materials behaved similarly to those of clinoptilolite, the higher the temperature, the lower its adsorption capacities.

In the case of the pumice matrix, it was founded that the materials modified with Al^{3+} present the highest removal capacities. Pumice is mainly formed by SiO_2 and its surface is integrated by silanol groups that are not very reactive and the $Al(OH)_3$ integrated to the structure is the responsible for fluoride removal, however, as describe before, modified pumice materials release a significant quantity of Al^{3+} to the aqueous medium, these materials could not be used to treat water.

According with the results, iron-modified materials are the best options for fluoride removal from aqueous solutions due to iron stability onto the mineral matrices and they have the lowest cost for their synthesis.

4. Conclusions

Fe^{3+} and Al^{3+} modified minerals were prepared by ion exchange and precipitation, the adsorbents have suitable textural properties and stability to guarantee fluoride removal from aqueous solutions. Metallic species interact with minerals in two different ways, in the case of Fe^{3+} it was possible to associate it with the structure by coordination with hydroxyl groups, while Al^{3+} is present as precipitate ($Al(OH)_3$) that is supported on minerals surfaces. In this last case aluminum was released into the aqueous solutions during the adsorption processes. Therefore aluminum-modified materials could not be used for water treatments. The incorporation of this chemical species favored the fluoride removal from water, by increasing both the surface specific area and affinity for fluoride ions. The adsorption of fluoride ions may take place by electrostatic attraction and ion exchange. Thermal treatments negatively influence the removal capacities due to the formation of metal oxides.

Acknowledgements

The authors are grateful to CONACYT for the financial support of this research, project 254665 and scholarship 415136 for NGCC.

References

[1] M. Habuda-Stanić, M. Ergović Ravančić, A. Flanagan, A review on adsorption of fluoride from aqueous solution, Materials 7 (2014) 6317–6366.
[2] M. Noori Sepehr, V. Sivansakar, M. Zarrabi, M. Senthil Kumar, Surface modification of pumice enhancing its fluoride adsorption capacity: an insight into kinetic and thermodynamic studies, Chem. Eng. J. 228 (2013) 192–204.
[3] G. Bia, C.P. De Pauli, L. Borgnino, The role of Fe(III) modified montmorillonite on fluoride mobility: adsorption experiments and competition with phosphate, J. Environ. Manage. 100 (2012) 1–9.
[4] S.H. Dolatshasi, M. Malakootian, H. Akbari, Acidity rate and fluoride content of consumed beverages in Kerman/Iran, J. Res. Health Sci. 9 (2009) 41–47.
[5] G. Asgari, B. Roshani, G. Ghanizadeh, The investigation of kinetic and isotherm of fluoride adsorption onto functionalize pumice stone, J. Hazard. Mater. 217-218 (2012) 123–132.
[6] K. Hosni, E. Srasra, Evaluation of fluoride removal from water by Hidrotalcite-Like compounds synthesized from kaolinic clay, J. Water Chem. Technol. 33 (2011) 164–176.
[7] WHO (World Health Organization), 3rd ed., Guidelines for Drinking-Water Quality 1 Recommendations, Geneva, 2008, pp. 306–308 incorporating 1st and 2nd addenda.
[8] V. Tomar, D. Kumar, A critical study on efficiency of different materials for fluoride removal from aqueous media, Chem. Central J. 7 (2013) 2–15.
[9] A. Salifu, B. Petruseski, K. Ghebremichael, L. Modestus, R. Buamah, C. Aubry, G.L. Amy, Aluminium (hydr)oxide coated pumice for fluoride removal from drinking water: synthesis, equilibrium, kinetics and mechanism, Chem. Eng. J. 228 (2013) 63–74.
[10] P. Loganathan, S. Vigneswaran, J. Kandasamy, R. Naidu, Defluoridation of drinking water using adsorption processes, J. Hazard. Mater. 248-249 (2013) 1–19.
[11] M. Malakootian, M. Javdan, F. Iranmanesh, Fluoride removal from aqueous solutions using bauxite activated mines in Yazd Province (case study: Kuhbanan water), J. Commun. Health Res. 3 (2014) 103–114.
[12] M. Malakootian, M. Javdan, F. Iranmanesh, Fluoride removal study from aqueous solutions using jajarm bauxite: case study on Koohbanan water, Res. Rep. Fluoride 48 (2015) 113–122.
[13] P. Miretzky, A. Fernandez Cirelli, Fluoride removal from water by chitosan derivates and composites: a review, J. Fluorine Chem. 132 (2011) 231–240.
[14] J.J. García-Sánchez, M. Solache-Ríos, J.M. Martínez-Gutiérrez, N.V. Arteaga-Larios, M.C. Ojeda-Escamilla, I. Rodríguez-Torres, Modified natural magnetite with Al and La ions for the adsorption of fluoride ions from aqueous solution, J. Fluorine Chem. 186 (2016) 115–124.
[15] M. Malakootian, M. Moosazadeh, N. Yousefi, A. Fatehizadeh, Flouride removal from aqueous solution by pumice: case study on Kuhbonan water, Afr. J. Environ. Sci. Technol. 5 (2011) 299–306.
[16] I. Díaz, Environmental uses of zeolites in Ethiopia, Catal. Today 285 (2017) 29–38.
[17] A. Vinati, B. Mahanty, S.K. Behera, Clay and Clay minerals for fluoride removal from water: a state-of-the-art review, Appl. Clay Sci. 114 (2015) 340–348.
[18] L. Gómez-Hortigüela, J. Pérez-Pariente, R. García, Y. Chebude, I. Díaz, Natural zeolites from Ethiopia for elimination of fluoride from drinking water, Sep. Purif. Technol. 120 (2013) 224–229.
[19] D. Baybaş, U. Ulusoy, Polyacrylamide–clinoptilolite/Y-zeolite composites: characterization and adsorptive features for terbium, J. Hazard. Mater. 187 (2011) 241–249.
[20] E. Donati, C.M. Polcaro, P. Ciccioli, E. Galli, The comparative study of a laccase-natural clinoptilolite-based catalyst activity and free laccase activity on model compounds, J. Hazard. Mater. 289 (2015) 83–90.
[21] L. Ma, Y. Xi, H. He, G.A. Ayoko, R. Zhu, J. Zhu, Efficiency of Fe–montmorillonite on the removal of Rhodamine B and hexavalent chromium from aqueous solution, Appl. Clay Sci. 120 (2016) 9–15.
[22] M.G. Martins, D.O.T.A. Martins, B.L.C. de Carvalho, L.A. Mercante, S. Soriano, M. Andruh, M.D. Vieira, M.G.F. Vaz, Synthesis and characterization of montmorillonite clay intercalated with molecular magnetic compounds, J. Solid State Chem. 228 (2015) 99–104.
[23] B. Heibati, S. Rodriguez-Couto, N. Gazme Turan, O. Ozgonenel, A.B. Albadarin, M. Asif, I. Tyagi, S. Agarwal, K. Gupta, Removal of noxious dye—Acid Orange 7 from aqueous solution using natural pumice and Fe-coated pumice Stone, J. Ind. Eng. Chem. 31 (2015) 124–131.
[24] D. Turan, C. Kocahakimoğlu, E. Boyaci, S.C. Sofuoglu, A.E. Eroğlu, Chitosan-immobilized pumice for the removal of As(V) from waters, Water Air Soil Pollut. 225 (2014) 1931–1943.
[25] Z. Sun, Y. Park, S. Zheng, G.A. Ayoko, R.L. Frost, Thermal stability and hot-stage Raman spectroscopic study of Ca-montmorillonite modified with different surfactants: a comparative study, Thermochim. Acta 569 (2013) 151–160.
[26] M. Malakootian, A. Fatehizadeh, N. Yousefi, Evaluating effectiveness of modified pumice in fluoride removal from water, Asian J. Chem. 23 (2011) 3691–3694.
[27] R.G. Pearson, Hard and soft acids and bases, Phys. Inorg. Chem. 85 (1963) 3533–3539.
[28] G. Biswas, M. Kumari, K. Adhikari, S. Dutta, A critical review on occurrence of fluoride and its removal through adsorption with an emphasis on natural minerals, Curr. Pollut. Rep. 3 (2017) 104–119.
[29] K. Gomoro, F. Zewge, B. Hundhammer, N. Megersa, Fluoride removal by adsorption on thermal treated lateritic soils, Bullet. Chem. Soc. Ethiopia 26 (2012) 361–372.
[30] D. Guaya, C. Valderrama, A. Farran, C. Armijos, J.L. Cortina, Simultaneous phosphate and ammonium removal from aqueous solution by a hydrated aluminum oxide modified natural zeolite, Chem. Eng. J. 271 (2015) 204–213.
[31] G. Vázquez Mejía, V. Martínez-Miranda, C. Fall, I. Linares-Hernández, M. Solache-Ríos, Comparison of Fe–Al-modified natural materials by an electrochemical method and chemical precipitation for the adsorption of F− and As(V), Environ. Technol. (2016) 37.
[32] G.C. Velázquez-Peña, M. Solache Ríos, V. Martínez-Miranda, Competing effects of chloride, nitrate, and sulfate ions on the removal of fluoride by a modified zeolitic tuff, Water Air Soil Pollut. 226 (2015) 22–36.
[33] A. Elkhalifah, M. Azmi Bustam, T. Murugesan, Thermal properties of different transition metal forms of montmorillonite intercalated with mono-, di-, and triethanolammonium compounds, J. Ther. Anal. Calorimetry 112 (2013) 929–935.
[34] S. Jevtić, I. Arčon, A. Rečnik, B. Babić, M. Mazaj, J. Pavlović, D. Matijaševic, M. Nikšić, N. Rajić, The iron(III)-modified natural zeolitic tuff as an adsorbent and carrier for selenium oxyanions, Microporous Mesoporous Mater. 197 (2014) 92–100.
[35] A. Brundu, G. Cerri, Thermal transformation of Cs-clinoptilolite to $CsAlSi_5O_{12}$, Microporous Mesoporous Mater. 208 (2015) 44–49.
[36] D.A. Almasri, T. Rhadfi, M.A. Atieh, G. McKay, S. Ahzi, High performance hydroxyiron modified montmorillonite nanoclay adsorbent for arsenite removal, Chem. Eng. J. 335 (2018) 1–12.
[37] A. Montes-Luna, N.C. Fuentes-López, Y.A. Perera-Mercado, O. Pérez Camacho, G. Ca struita-de León, S.P. García Rodríguez, M. García-Zamora, Caracterización de clinoptilolita natural y modificada con Ca^{2+} por distintos métodos físico-químicos para su posible aplicación en procesos de separación de gases, Superficies y vacío 28 (2015) 5–11.
[38] F. Lin, G. Zhu, Y. Shen, Z. Zhang, B. Dong, Study on the modified montmorillonite

for adsorbing formaldehyde, Appl. Surf. Sci. 356 (2015) 150–156.
[39] A. Rapacz-Kmita, M.M. Bućko, E. Stodolac-Zych, E. Mikołajcz, P. Dudek, M. Trybus, Characterisation, *in vitro* release study, and antibacterial activity of montmorillonite-gentamicin complex material, Mater. Sci. Eng. C 70 (2017) 471–478.
[40] L. Borgino, M.J. Avena, C.P. De, Pauli, Synthesis and characterization of Fe(III)-montmorillonites for phosphate adsorption, Colloids Surf. A: Physicochem. Eng. Asp. 341 (2009) 46–52.
[41] S. Seraj, R.D. Ferron, M.C.G. Juenger, Calcining natural zeolites to improve their effect on cementitious mixture workability, Cement Concrete Res. 85 (2016) 102–110.
[42] G. Biswas, M. Dutta, S. Dutta, K. Adhikari, A comparative study of removal of fluoride from contaminated water using shale collected from different coal mines in India, Environ. Sci. Pollut. Res. 23 (2016) 9418–9431.